AHARONOV-BOHM-TYPE EFFECTS IN ANTIDOT ARRAYS AND THEIR DECOHERENCE

MASANORI KATO, HIROYASU TANAKA, AKIRA ENDO, SHINGO KATSUMOTO AND YASUHIRO IYE

Institute for Solid State Physics, University of Tokyo, 5-1-5 Kashiwanoha Kashiwa, Chiba 277-8581 Japan

We have investigated the Aharonov-Bohm(AB)-type quantum oscillations in triangular and square arrays of antidots fabricated from two-dimensional electron systems in GaAs/AlGaAs heterostructure.

Keywords: Aharonov-Bohm oscillation, two-dimensional electron system, antidot array; vortex glass transition, GaAs/AlGaAs

1. Introduction

Since its first experimental observations[1,2], the Aharonov-Bohm (AB) effect in electron transport has been extensively studied in a wide range of mesoscopic conductors not only in the diffusive metallic transport regime but also in the ballistic (or semi-ballistic) transport regime realized in high mobility two-dimensional electron system (2DES) in semiconductor heterostructures.

The AB effect is a manifestation of quantum interference effect and shows up as oscillatory resistance of a ring-shaped sample at low temperatures as a function of external magnetic field. It is customary to distinguish two types of the AB effect: The Altshuler-Aronov-Spivak (AAS) effect ($h/2e$ oscillation) is attributed to interference of a time-reversed pair of electron waves. As long as the spin-orbit effect is small, the AAS interference is always constructive at zero magnetic field. By contrast, the phase of the AB interference (in its narrower sense), which is responsible for h/e oscillation, is sample specific. This fundamental difference is highlighted in an assembly of identical rings. While the AB interference effect tends to be smeared by the random phase averaging in such a system, the AAS effect is immune to the ensemble averaging, as demonstrated experimentally[3].

Antidot lattices fabricated from 2DES constitute another interesting class of systems to study the AB effect. An antidot lattice can be viewed as a network consisting of many rings. The first observation of the AB oscillation in antidot lattice was made by Nihey *et al.*[4] and by Weiss *et al.*[5] They detected *B*-periodic small oscillations superposed on the commensurability peak of magnetoresistance in square antidot lattices. Later, the AAS oscillation was observed in triangular antidot lattice[6].

When one was reminded that dephasing of the AB interference should occur in an array of rings due to ensemble averaging, the very fact that AB oscillation could be observed in antidot lattice of macroscopic overall size, was rather surprising. Subsequent theoretical studies have attributed the effect to oscillatory fine structure of the density of state spectra, as calculated, for instance, by periodic orbit theory. For this reason, it is customary to call the effect AB-"type" oscillation so as to distinguish it from the ordinary AB effect in the single ring case. There is an intermediate case of finite antidot lattices[7], in which a small number of antidots constitute a mesoscopic size system that becomes phase coherent as a whole at low enough temperatures.

Despite a great deal of the theoretical efforts[8], full understanding of the physical

origin of the AB-type oscillation in macroscopic antidot lattice is yet to be worked out.

We have investigated the AAS and AB-type oscillations in triangular and square antidot lattices both near zero magnetic field and in high fields. Due to the page limitation, we focus on the low field behavior in this paper. Various aspects of the AB-type oscillation effect in the quantum Hall regime are discussed elsewhere[9,10].

2. Experiment

The samples used in the present study were fabricated from a GaAs/AlGaAs single heterostructure wafer with electron density n= 3.8x10^{15} m^{-2} and mobility μ= 60 m^2/Vs. Using electron beam lithography and shallow wet etching, triangular and square arrays of antidots as shown in the inset of Fig. 1 were fabricated on the active area of Hall bar samples with AuGe/Ni Ohmic contact pads. The lattice period was a= 1 μm and the antidot diameter was d= 600nm. Because of the depletion region of width ~100nm around each dot, the effective antidot diameter becomes d*~800nm, leaving the effective width of the narrowest part of the channel between the antidot ~100nm. The 2DES density was controlled by a Au–Ti Schottky front gate, which also changed the effective channel width. For the "large" array samples the total number of antidots was ~10^4, while for the "small" array samples it was ~50.

Transport measurements were made by a standard ac lock-in technique at 13Hz. The sample was directly immersed in the ^{3}He-^{4}He mixture of the mixing chamber of a dilution refrigerator at a base temperature 30mK. Magnetic fields up to 15 T were applied perpendicular to the 2DES plane.

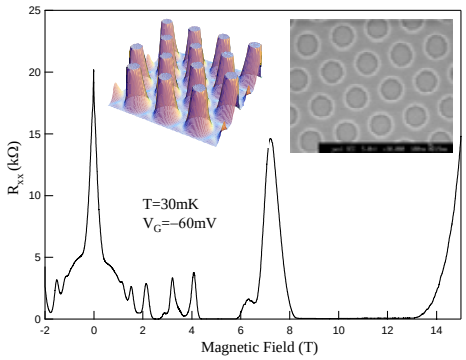

Figure 1. *Inset*: The left figure is a schematic potential landscape for electrons in an antidot lattice. The right panel shows an SEM image of the triangular lattice of antidots. The lattice constant is a= 1 μm and the antidot diameter is d= 600nm. *Main Panel*: Magnetoresistance at 30mK.

3. Results and Discussions

The main panel of Fig. 1 shows the magnetoresistance trace of the large array triangular lattice sample. The effect of the antidot array is most prominent in the enhancement of zero-field resistance and the large negative magnetoresistance in the low field range. By contrast,, the overall shape of the magnetoresistance trace in the high field regime, *i.e.* the Shubnikov-de Haas oscillation and the quantum Hall effect, is not so different from those of unpatterned 2DES samples. However, when the fine details of the trace exhibits different kinds of oscillatory behavior.

The inset of Fig. 2 is an expanded view of the peak at zero field of the trace in Fig.1, which clearly shows oscillatory behavior. In order to highlight the oscillatory part, the low field magnetoresistance with the smooth background subtracted, are shown in the main panel. Oscillations with two distinct frequencies are readily recognized. The rapid oscillation at around zero magnetic field has a period $h/2eS$=2.6mT ($S = \left(\sqrt{3}/2\right)a^2 = 0.80\,\mu\text{m}^2$ being the unit cell area of the triangular lattice) and has a maximum at zero magnetic field, so it is identified as the AAS oscillation.

The smaller amplitude oscillation at somewhat higher field has a period h/eS=5.2mT, and is the AB-type oscillation.

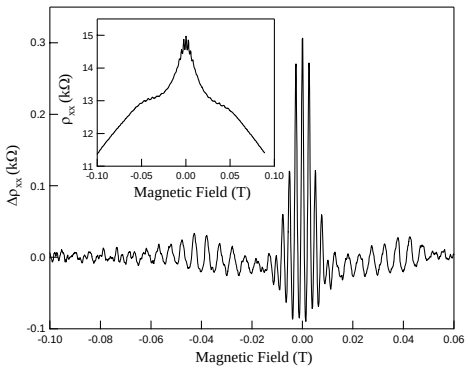

Figure 2. *Inset*: Magnetorestance traces of the triangular lattice sample at low magnetic field. *Main Panel*; The oscillatory part of the magnetoresistance highlighted by subtracting the smooth background. The AAS ($h/2e$) and the AB-type (h/e) oscillations are clearly identified.

Similar phenomena were also observed in the square lattice samples. It is worth noting that the earlier studies[4-6] have reported that the low field magnetotransport behavior is quite different between the square and the triangular antidot lattices. For instance, the AAS oscillation was observed only in the latter, and the former showed a slightly positive magnetoresistance with a "matching" peak while a large negative magnetoresistance characterized the latter. These differences have been attributed to the fact that the ballistic electron trajectories tend to be more strongly back-scattered in the triangular lattice than the square lattice. While such differences in behavior is manifest among samples with small to intermediate values of aspect ratio, the difference tends to diminish for systems with larger aspect ratios (*i.e.* narrower channel) such as those studied here.

In order to study the decoherence mechanisms in these systems, we measured the temperature dependence of the amplitude of the AAS and AB oscillations. Figure 3 shows the temperature dependence of the AAS oscillation observed in the square lattice sample. The data can be fitted to the following functional form reflecting the temperature dependence of the inelastic scattering time $\tau \propto T^{-p}$.

$$A_{\mathrm{AAS}} \propto \exp\left(-\alpha T^{p}\right) \qquad (1)$$

with p~1.6. Our earlier study[9] on triangular lattices have yielded a similar exponent p~1.5 and 1.1.

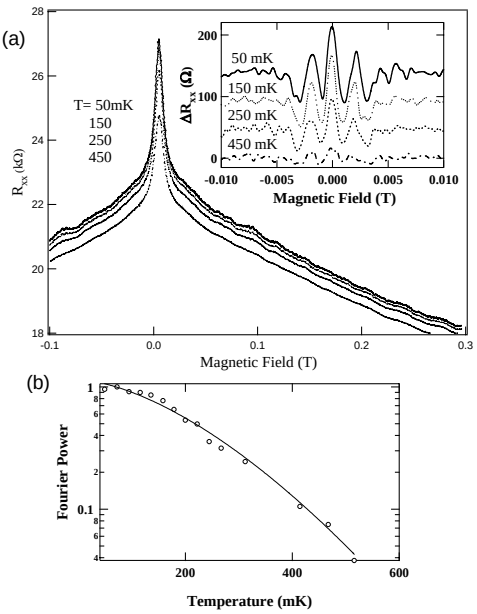

Figure 3. (a) Magnetorestance traces of the square antidot lattice sample at different temperatures. The inset shows the AAS ($h/2e$) oscillation around zero magnetic field. (b) Temperature dependence of the AAS oscillation. The solid curve is a fit to the functional form $\exp(-\alpha T^{p})$

The AB-type oscillation in antidot arrays is attributed to oscillatory fine structure in the density of states of the system[8], and its temperature dependence is expected to arise from temperature smearing of the density-of-state feature. Figure 4 shows the AB-type oscillation in the square lattice sample at low magnetic fields. The temperature dependence of the amplitude in this case is fitted to the functional form

$$A_{\mathrm{AB}} \propto \frac{aT}{\sinh(aT)}, \qquad a = \frac{2\pi^2 k_{\mathrm{B}}}{\Delta E}, \qquad (2)$$

which is shown by the solid curve. In our earlier study on triangular lattice samples, we found that the experimental results show some deviation from the above functional form, *i.e.* saturation of AB-type oscillation amplitude for $T \to 0$ was found to be slower than eq.(2). We attributed it to the temperature dependence of the phase coherent area[9]. The present result on the square lattice is somewhat at variance with the previous result, and appears to be explained rather simply by thermal smearing. The origin of the different experimental outcome is unknown at the moment.

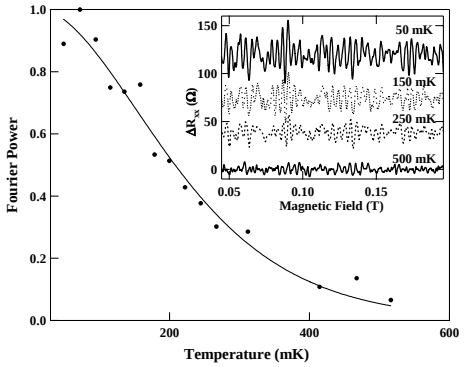

Figure 4. *Inset*: The AB-type oscillation in the square antidot lattice sample. *Main panel*: The temperature dependence of the amplitude, the solid curve represents a fit to a functional form $aT/\sinh(aT)$.

4. Conclusion

We have studied quantum coherent oscillatory phenomena in antidot arrays with triangular and square symmetries. The difference in the lattice symmetry becomes less important for antidot arrays with larger aspect ratios. The temperature dependence of the AAS oscillation reflects that of the inelastic scattering time. On the other hand, the temperature dependence of the AB-type oscillation is understood in terms of thermal smearing of oscillatory fine structure in the density of states.

Acknowledgements

The work is supported in part by Grant-in-Aid for Scientific Research from the Ministry of Education, Culture, Sport, Science and Technology (MEXT), Japan.

References

1. D.Yu. Sharvin and Yu.V. Sharvin: Pis'ma Zh. Eksp. Theor. Fiz. 34 (1981) 285. [JETP Lett. 34 (1981) 272.]; B.L. Altshuler, A.G. Aronov and B.Z. Spivak: Pis'ma Zh. Eksp. Theor. Fiz. 33 (1981) 101. [JETP Lett. 33 (1981) 94.]
2. R.A. Webb, S. Washburn, C.P. Umbach and R.B. Raibowitz: Phys. Rev. Lett. 54 (1985) 2696.
3. C.P. Umbach, C. van Haesendonck, R.B. Laibowitz, S. Washburn and R.A. Webb: Phys. Rev. Lett. 56 (1986) 386.
4. F. Nihey and K. Nakamura: Physica B 184 (1993) 398.
5. D. Weiss, K. Richter, A. Menshing, R. Bergmann, H. Schewzer, K. von Klitzing and G. Weimann: Phys. Rev. Lett. 70 (1993) 4118.
6. F. Nihey, S.W. Hwang and K. Nakamura: Phys. Rev. B 51 (1995) 4649.
7. R. Schuster, K. Ensslin, D. Wharam, S. Kuehn, J.P. Kotthaus, G. Boehm, W. Klein, G. Traenkle and G. Weimann: Phys. Rev. B 49 (1994) 8510.
8. S. Ishizaka, F. Nihey, K. Nakamura, J. Sone and T. Ando: Phys. Rev. B 51 (1995) 9881; S. Uryu and T. Ando: Phys. Rev. B 53 (1996) 13613.
9. Y. Iye, M. Ueki, A. Endo and S. Katsumoto, J. Phys. Soc. Jpn. 73 (2004) 3370.
10. M.Kato, H.Tanaka, A.Endo, S.Katsumoto and Y.Iye, to appear in the Proceedings of EP2DS-16; M. Kato, H. Tanaka, A. Endo, S. Katsumoto and Y. Iye, to appear in the Proceedings of LT24.